Elsevier Editorial System(tm) for Construction & Building Materials

Manuscript Draft

Manuscript Number: CONBUILDMAT-D-16-05112R1

Title: OPTIMIZATION OF THE ALKALI ACTIVATION CONDITIONS OF GROUND GRANULATED SiMn SLAG

Article Type: Research Paper

Keywords: SiMn slag; alkali activation; pastes; waterglass

Corresponding Author: Mr. Emilio Zornoza, Chemistry

Corresponding Author's Institution: Universidad de Alicante

First Author: Rosa Navarro

Order of Authors: Rosa Navarro; Emilio Zornoza, Chemistry; Pedro Garcés; Isidro Sánchez; Eva G Alcocel

Abstract: The viability of using a SiMn slag as raw material for the preparation of alkali activated binder has been analysed. The slag has been characterized from the physical, chemical, mineralogical and microstructural point of view. The solution used for the alkali activation process was waterglass, which was prepared by the mix of a sodium silicate solution with sodium hydroxide. The influence of the following design parameters in alkali activated pastes has been studied: %Na2O, SiO2/Na2O ratio and activating solution/slag ratio. All the prepared specimens have been cured under a 100% of relative humidity atmosphere and no additives have been included in the formulations. For the evaluation of the alkali activation process a response surface methodology has been adopted by modelling the obtained results for different control parameters. The proposed experimental methodology consisted of a composite cubic-type experimental design which follows 2nd degree polynomial model. The control parameters of the pastes used in this research have been: workability, compressive strength at 7, 28 and 90 days of curing time, setting times and shrinkage at 50% of relative humidity. The results show that it is possible to valorise the SiMn slag through its use as an alkali activated binder. In general, workability decreases as the %Na2O increases and SiO2/Na2O ratio decreases. Initial setting times ranges from 38 to 263 min depending on the activating solution composition, and workability time decreases for increasing %Na2O. A compressive strength higher than 45 MPa can be achieved by the following activating conditions: 4.0-4.5%Na2O, SiO2/Na2O = 1.00 and activating solution/slag = 0.35-0.375. Shrinkage values of pastes that were cured at 50% of relative humidity ranged from 1.5% to 3.0%.

Cover Letter

Dr Emilio M. Zornoza Gómez
Departamento de Ingeniería Civil
Universidad de Alicante
Tel: (96) 5903707 Fax: (96) 5903678
email: emilio.zornoza@ua.es

December, 13th 2016

Dear Editor,

We enclose the manuscript of the paper entitled "OPTIMIZATION OF THE ALKALI ACTIVATION CONDITIONS OF GROUND GRANULATED SiMn SLAG" by R. Navarro et al., for refereeing and, if the case warrants it, publishing in the Journal "CONSTRUCTION AND BUILDING MATERIALS".

Yours sincerely

Dr. Emilio Zornoza

***Detailed Response to Reviewers**

The authors would like to thank the reviewer's comments. Thanks to their valuable suggestions the manuscript has been greatly improved. The paper has been revised completely and the English has been edited as requested. Also, the following aspects have been clarified:

Reviewer #1:

1. First the all, this paper should be written according to the journal criteria.

Several changes have been made in the manuscript in order to fulfil the journal criteria: include keywords after the abstract, line and page numbering, position of table captions,

2. Source writing in the text should be corrected.

Source writing has been changed to 11 points Times New Roman (except in tables, in which a 10 point size has been used) and normal space between characters.

3. The relevant information on the shrinkage of hardened pastes should be included in the summary and conclusion part.

The following text has been added to the abstract:

> "Shrinkage values of pastes that were cured at 50% of relative humidity ranged from 1.5% to 3.0%."

The following text has been included in the conclusions:

> "High shrinkage values have been registered for all pastes in the 50% RH ambient. In these conditions, shrinkage achieves a stable value after 30 days. Shrinkage levels have ranged from 1.5% to 3.0% approximately and its maximum value is observed for s/s ratio around 0.38 and 4.5% Na_2O in pastes with Ms = 1.00."

4. The English writing should be greatly improved. In the following examples, word errors

We apologize for the high number of grammatical errors that have been included in the text. Many of them are just a consequence of a lack of attention in the manuscript elaboration. The new version of the manuscript has been carefully revised.

Reviewer #2:

1. This article should be discussed by studying different aspects with previous studies. The results and the discussion part should be better enriched.

We would highly appreciate that this reviewer could express the suggestion more accurately. In our opinion the manuscript includes a high amount of results and they have been discussed according to the most actual references in the state-of-the-art. In fact, the extension of the manuscript exceeds the maximum number of pages that is recommended by the journal.

Reviewer #3:

1. In the abstract: "….. sodium hydroxide (waterglass)….." is not right and must be modified.

We are not indicating that sodium hydroxide is waterglass, but a solution prepared by the mix of sodium silicate and sodium hydroxide. In general, waterglass is a solution of sodium and silicate but not the stoichiometric compound Na2SiO3. When waterglass is prepared, different SiO2/Na2O ratios can be defined and the way to do it is to mix sodium silicate with sodium hydroxide.

To avoid the misunderstanding we have rewritten the sentence in the following way:

“The solution used for the alkali activation process was waterglass, which was prepared by the mix of a sodium silicate solution with sodium hydroxide”

2. The abstract should focus on the main results obtained in the study especially the influence of significant factors on the workability, compressive strength, setting time and shrinkage of pastes.

The abstract has been modified to include the main results reported in the manuscript. The following sentences have been inserted in the summary:

“In general, workability decreases as the %Na2O increases and SiO2/Na2O ratio decreases.”

“Initial setting times ranges from 38 to 263 min depending on the activating solution composition, and workability time decreases for increasing %Na2O.”

“Shrinkage values of pastes that were cured at 50% of relative humidity ranged from 1.5% to 3.0%.”

3. There are many grammatical errors in the manuscript, which should be modified.

We apologize for the high number of grammatical errors that have been included in the text. Many of them are just a consequence of a lack of attention in the manuscript elaboration. The manuscript has been carefully revised.

4. The reference of some sentences must be mentioned in the manuscript:

- **In the silico-manganese production process, 0,9-2,2 tons of slags are discharged to produce 1 ton of silico-manganese.**
- **In Spain, near 200,000 ton/year of silico-manganese alloy are produced and the total production of SiMn slag is about 350,000 tons per year, so the amount is high enough to propose its reuse and valorisation.**

These particular data came from a Technical Guide published by the Spanish Ministry of Industry and Energy, in Spanish. In order to provide a more useful information and also an accessible reference we have replaced those sentences by the following:

“The global production of silico-manganese alloy in year 2016 was 12.5 million tons [5]. Typically the slag generation is about 1.2–1.4 tons for every ton of SiMn alloy produced [6] thus the slag generated is in the tune of 15.0–17.5 million tons per year, so the amount is high enough to propose its reuse and valorisation.”

5. Many sentence are not clear for the readers and must be modified;

- "In addition, it has been demonstrated [11] the effectiveness of the mechanical activation of the air-cooled SiMn slag on the pozzolanic behaviour."

That sentences has been rewritten in the following sense:

“Allahverdi et al. concluded that the air-cooled SiMn slag exhibits relatively low to moderate pozzolanic and latent hydraulic properties which can be improved by mechanical activation of the slag [13].”

- **"Initial setting time and setting time were significantly reduced by ……..."**

Initial setting time refers to the time taken by the sample from its preparation to the beginning of setting process. Setting time (also called workability time) refers to the time that it takes from the beginning to the end of the setting process. In order to clarify the sentence it has been substituted by the following one:

“The overall setting process could significantly accelerated by the mechanical activation procedure in the following order: ball milling (slower), the attrition milling (intermediate) and vibration milling (faster).”

- **SiMn slag was activated using different solutions of waterglass.**

That sentence has been rewritten in the following way:

“Alkali activation procedure has been successfully applied to SiMn slag for pastes preparation using waterglass as alkaline activator”

6. The reason(s) of some results are not presented in the manuscript:

- **For given s/s ratio, the fluidity of paste increases as %Na2O is increased up to a certain percentage, and then it drops if %Na2O continues increasing.**

All results used as discussion arguments are presented in the manuscript. The sentence you are mentioning alludes to Figure 6, in which it can be observed an increase in fluidity up to a certain value and then a decrease when we move horizontally from left to right at any y-value of the graph.

- **Mechanical strength obtained with waterglass as activator are higher than NaOH as activator.**

That statement arises from the comparison of present manuscript results with other authors’ findings. This comparison would agree with other works which indicate that waterglass is better activator from the mechanical performance point of view, highlighting the important role played by silicate ions in the activating solution [38,45].

Nevertheless, we agree with the reviewer and the sentence does not deserve to be included in the conclusions, so we have removed it.

7. Recently, many papers related to alkali activated slag have been published in the Journal of Construction & Building Materials. You should use some of these paper in the references.

In our opinion we have included the most relevant references in relation to the results of the manuscript. It is true that CBM contains lots of information about alkali activated slag but most of them deals with blast furnace slag. SiMn slag has some things in common with blast furnace slag but many differences as well. Finally, 57 references have been used in the paper, and that includes 6 from CBM. Obviously, if the reviewer knows any reference that should be added to the manuscript we would consider the convenience of its inclusion.

***Highlights**

- Alkali activation with waterglass has been successfully applied to SiMn slag.
- The paste fluidity depends on the $\%Na_2O$ and SiO_2/Na_2O ratio.
- A compressive strength higher than 45 MPa can be achieved for pastes.
- Shrinkage levels of pastes have ranged from 1.5% to 3.0% approximately in 50% RH.

OPTIMIZATION OF THE ALKALI ACTIVATION CONDITIONS OF GROUND GRANULATED SiMn SLAG

R. Navarro[1], E. Zornoza[1], P. Garcés[1], I. Sánchez[1], E.G. Alcocel[2]

1. *Dept. of Civil Engineering. University of Alicante (Spain)*
2. *Dept. of Architectonic Constructions. University of Alicante (Spain)*

ABSTRACT

The viability of using a SiMn slag as raw material for the preparation of alkali activated binder has been analysed. The slag has been characterized from the physical, chemical, mineralogical and microstructural point of view. The solution used for the alkali activation process was waterglass, which was prepared by the mix of a sodium silicate solution with sodium hydroxide. The influence of the following design parameters in alkali activated pastes has been studied: $\%Na_2O$, SiO_2/Na_2O ratio and activating solution/slag ratio. All the prepared specimens have been cured under a 100% of relative humidity atmosphere and no additives have been included in the formulations. For the evaluation of the alkali activation process a response surface methodology has been adopted by modelling the obtained results for different control parameters. The proposed experimental methodology consisted of a composite cubic-type experimental design which follows 2^{nd} degree polynomial model. The control parameters of the pastes used in this research have been: workability, compressive strength at 7, 28 and 90 days of curing time, setting times and shrinkage at 50% of relative humidity. The results show that it is possible to valorise the SiMn slag through its use as an alkali activated binder. In general, workability decreases as the $\%Na_2O$ increases and SiO_2/Na_2O ratio decreases. Initial setting times ranges from 38 to 263 min depending on the activating solution composition, and workability time decreases for increasing $\%Na_2O$. A compressive strength higher than 45 MPa can be achieved by the following activating conditions: 4.0-4.5%Na_2O, SiO_2/Na_2O = 1.00 and activating solution/slag = 0.35-0.375. Shrinkage values of pastes that were cured at 50% of relative humidity ranged from 1.5% to 3.0%.

Keywords: SiMn slag; alkali activation; pastes; waterglass

1. INTRODUCTION

Cement production industry can be considered responsible of 6-7% of total CO_2 emissions to the atmosphere [1] and the consumption of 2-3% of the primary energy produced worldwide [2]. Our society has the challenge of reducing both energy demand and CO_2 emissions, and for that reason it is necessary to seek alternative binders with competitive properties in the field of civil engineering and building materials, that is, comparable to Portland cement. On the other hand, from an environmental point of view, the strategy of using binders with a lower demand of natural resources and energy can be also supported with the other complementary actions. These actions could involve the reuse of industrial by-products or wastes, with the aim of reducing the extraction of raw materials in quarries and the accumulation of wastes in dumping sites [2–4]. In this research, the waste material whose valorisation is proposed as raw material to design an ecological binder is a SiMn slag generated in the production of silico-manganese iron alloys. The global production of silico-manganese alloy in year 2016 was 12.5 million tons [5]. Typically the slag generation is about 1.2–1.4 tons for every ton of SiMn alloy produced [6] thus the slag generated is in the tune of 15.0–17.5 million tons per year, so the amount is high enough to propose its reuse and valorisation. This SiMn slag presents a silico-calcic nature similar to blast furnace slag, but with a different chemical composition: lower content of CaO and a significantly high proportion of MnO.

At present, most published researches about this slag have been focused on its pozzolanic properties, and have proposed its valorisation as cementing material replacing different percentages of Portland cement. The first reference found about this type of application dates from 1999 [7]. This work revealed that the presence of MnO in the slag may delay the initial development of the pozzolanic reaction, but this trend changed in the long term and even a clearly positive effect was observed in the compressive strength. Other studies about SiMn slag [8–11] highlighted the aforementioned observation: replacing Portland cement by SiMn slag in quantities up to 30% offered lower mechanical strength than control samples for curing ages lower than 28 days. From 90 days of curing time, no significant differences were observed in this parameter. About the quality of the cementing products produced by the pozzolanic reaction of SiMn slag, a similar chemical resistance was observed when exposed to seawater, 0.5 M NaCl and 0.5 M Na_2SO_4 solutions to that one shown by cement Portland samples [10].

Another scientific work about slags with different proportions of MnO concluded that a content of MnO higher than ~33% was not suitable as supplementary cementing materials due to its detrimental effect and

highlighted the important role played by the slag cooling process type (air-cooled or granulated) in its reactivity [12]. Allahverdi et al. concluded that the air-cooled SiMn slag exhibits relatively low to moderate pozzolanic and latent hydraulic properties which can be improved by mechanical activation of the slag [13]. This type of procedures increased the quantity of cement replacement that could be used up to 35%. Other authors [14] proposed the use of the granulated SiMn slag as source of silicon for the tobermorite production through hydrothermal reaction in autoclave curing conditions. They concluded that the best mechanical behaviour was offered by samples with 17% of Portland cement and 83% of SiMn slag with a molar ratio $CaO/SiO_2 = 1$.

Besides, it is well known that chemical procedures such as alkali activation have enhanced the development of more efficient cementing matrix and avoid the use of Portland cement [1,2,15–19]. Alkali activated cement generically refers to a wide group of binders that solidify after the attack of highly alkaline solution to a reactive solid [18]. In the last years an exponential growth of the number of researches related to this type of alternative binders has occurred, and at present they are gaining true technological significance [20]. As a results of this tendency, not only benefits in terms of lower energy consumption and reduced environmental impact have been observed [21–24], but also good mechanical behaviour [25,26] and durability [27,28]. Nevertheless, characteristics of alkali activated binders strongly depend on the original material and activation conditions [1,29]. There exists a wide variety of solid substrates that have been successfully activated through this type of procedure. Among the most studied materials it can be found blast furnace slags and different pozzolanic materials: fly ash, natural pozzolans, metakaolin, glass waste and in a lesser extent other slags from iron and steel industry, and other industrial by-products [1,30,31].

Chemical, mineralogical and pozzolanic characteristics presented by the SiMn slag enable its use for obtaining alkali activated materials. Kumar et al. [6] studied the effect of the mechanical activation of the slag in the activation process, and it was evidenced the potential of the SiMn slag to be activated with a sodium hydroxide. Previously to the chemical process, the SiMn slag was treated mechanically by different procedures (ball milling, attrition milling and eccentric vibratory milling). As a result, different particle size distributions and different reactivity due to physico-chemical changes in the mass and the surface of the particles were obtained. The processes did not change the general chemistry of the material. The overall setting process could be significantly accelerated by the mechanical activation procedure in the following

order: ball milling (slower), the attrition milling (intermediate) and vibration milling (faster). A similar behaviour was observed for the compressive strength after 28 days of curing time: 24 MPa for ball milling samples, 66 MPa for attrition milling specimens and 101 MPa for vibration milling conditions. The conclusion was that the reactivity of the slag was improved by the mechanical activation and it depends on the type of milling used. It was proposed the following order of reactivity: vibration milling, attrition milling and ball milling. The mechanical strength obtained for specimens prepared with eccentric vibration milling were better than those values presented by blast furnace slags or other similar products [32]. However, other authors [31] considered that the high-energy milling was responsible for achieving this performance, as the strength reached through this process was more than three times the strength achieved through alkali-activation of the same slag processed through a regular ball-milling process.

Other investigations conducted upon other alkali activated wastes have demonstrated that microstructure and properties of pastes directly depend on the type of activator [33,34]. The aim of this research is to optimize the alkali activation process of the ground granulated SiMn slag using as activator waterglass prepared by the mix of a sodium silicate solution with sodium hydroxide. For that reason, the slag has been characterized from the chemical, physical, mineralogical and microstructural point of view. The design parameters that have been used as independent variables of the optimization procedure are the following: $\%Na_2O$: concentration of the solution, SiO_2/Na_2O ratio: modulus of sodium silicate solution (Ms), and alkaline activator solution/slag mass ratio (s/s ratio). Alkali activated pastes have been fabricated and the following parameters have used to evaluate their performance: workability, setting times, compressive strength and shrinkage. Statistical techniques of experimental design have been applied to evaluate the influence on the activation process and the development of technological properties of the binder that support its subsequent application in the fabrication of mortars. In order to show a better understanding of how the dosage variables affect the properties that have been controlled in this research, an analysis by Response Surface Method (RSM) has been implemented. This methodology is a statistical development for design of experiments which allows to obtain an optimization of the variables under study and their relative effect on the selected response parameters [35,36].

2. EXPERIMENTAL

2.1 SiMn slag and alkaline activators

The primary raw material used was a SiMn slag from the Ferroatlántica plant sited at Boo de Guarnizo (Cantabria, Spain). Table 1 shows the results of the chemical analysis obtained by X-ray fluorescence. According to the slag basicity index (CaO/SiO_2 = 0.80 and $(CaO+MgO)/(SiO_2+Al_2O_3)$ = 0.73) and hydraulicity index ($(CaO+0.5MgO+Al_2O_3)/(SiO_2+MnO)$ = 0.85), this residue can be classified as an acid slag with moderate hydraulicity [7,37,38].

Component	SiO_2	CaO	MnO	Al_2O_3	MgO	Fe_2O_3	K_2O	Na_2O	SO_3	Cl	BaO	P_2O_5	SrO	TiO_2	ZrO_2	L.O.I.
Mass % as oxide	36.53	29.10	12.23	9.86	4.69	0.92	1.08	0.34	2.77	0.16	1.60	0.35	0.14	0.19	0.04	-1.25

Table 1. Composition of the SiMn slag determined by X-ray fluorescence analysis.

The determination of crystalline phases and the vitreous phase content by X-ray diffraction have been performed in a PANalytical diffractometer, model EMPYREAN. The complete identification and quantification have been determined by Rietveld method [39] using quartz as standard sample, $MoK_{\alpha 1}$ radiation, a scan from 3 to 35 degrees, for 5 hours in 0.0113 degrees steps, at 50 kV and 50 mA. Two different slag samples were analysed, each one of them with a different cooling process in the production plant: air-cooled and water-cooled (granulated). Table 2 presents the results obtained in the X-ray diffraction analysis the both SiMn slag samples.

(%± s)	Alabandite (MnS)	Augite ($CaMg(SiO_3)_2$)	Graphite (C)	Vitreous
Air-cooled SiMn slag	2.3±0.1	21.4±0.3	--	76.3±0.7
Granulated SiMn slag	2±1	--	2±1	96±1.5

Table 2. Results of the X-ray diffraction analysis of SiMn slag samples. (s: standard deviation)

The granulated SiMn slag presented higher vitreous materials than air-cooled slag. For that reason, all the specimens fabricated in this research were prepared with the granulated one.

Table 3 shows the results of the determination of reactive silica and insoluble residue of the SiMn slag according to standards UNE 80225-2012 and UNE 196-2-2014 [40,41].

Insoluble residue	Total %SiO_2	SiO_2 insoluble residue	Reactive SiO_2
3.35%	36.53%	2.73%	33.80%

Table 3. Reactive silica and insoluble residue of the SiMn slag.

133 The slag chemical composition shows a total content of silicon, calcium and aluminium oxides about 76% of
134 the material. In addition, a relatively high content of reactive silica and a significantly high vitreous phase
135 proportion are observed in the sample. Therefore, according to these data, SiMn slag presents a set of
136 characteristics that make it suitable to be alkali-activated [37,42].

137 Previous studies about the same waste material conducted by other authors showed a 35% of reactive silica,
138 and the presence of free CaO or MgO that may produce expansive processes [8]. In present research, no free
139 CaO and MgO were detected in the slag composition. With regard to the possibility of releasing toxic
140 substances, bibliographic data show that the elemental composition of the SiMn slag (major and minor
141 compounds) is similar to the one held by Portland cement, and consequently, the presence of additional toxic
142 elements was not detected.

143 In a reference to other parameters which significantly affect the reactivity, SiMn slag has been characterized
144 by the determination of its fineness according to Blaine's air permeability method [43]. Also, particle size
145 distribution of the slag has been measured by a laser diffraction equipment, using a Malvern Instruments,
146 model Mastersizer 2000. The slag was ground in dry conditions using a laboratory ball mill Nanneti model
147 SPEEDY 1 for 25 minutes. For that reason, SiMn slag particles offer irregular shape, which will be related to
148 fresh state behaviour, water demand and final porosity of prepared pastes [44]. The Blaine's fineness after
149 grinding was 5512 cm^2/g and ground slag particle size distribution offered the following characteristic
150 values: D_{50} = 9.2 µm and $D_{4,3}$ = 15.2 µm. Other authors have established that the optimal fineness of the
151 material for the alkali activation process depends on the particular slag, nature of the activator and curing
152 conditions, and there exists a fineness optimal range between 4500-6000 cm^2/g for acid slags similar to the
153 one investigated in present research [38].

154 Alkaline solutions used to activate the SiMn slag were waterglass prepared with a commercial sodium
155 silicate (Na_2SiO_3 (neutral solution QP, Panreac): SiO_2/Na_2O molar ratio = 3.28) and sodium hydroxide
156 (technical grade, Panreac).

$\%Na_2O$	**Ms**	**s/s ratio**	**Density (g/cm^3)**	**pH**	**Conductivity (mS)**
4	0.75	0.35	1.23	13.22	164
4	0.75	0.45	1.18	13.24	168
4	1	0.35	1.26	13.66	125.6
4	1	0.375	1.25	13.69	129.6

4	1	0.4	1.22	13.71	131.5
4	1.25	0.35	1.29	13.25	84.9
4	1.25	0.45	1.21	13.38	93.6
4.5	1	0.35	1.3	13.62	112.2
4.5	1	0.375	1.27	13.65	121.1
4.5	1	0.4	1.26	13.68	126.4
5	0.75	0.4	1.26	13.12	156.7
5	1	0.35	1.33	13.54	99.5
5	1	0.375	1.3	13.61	110.4
5	1	0.4	1.3	13.64	117.4
5	1	0.45	1.25	13.33	118.1
5	1.25	0.4	1.31	13.37	76.5
6	0.75	0.35	1.38	12.8	102.7
6	0.75	0.45	1.28	13.23	151.6
6	1	0.4	1.36	13.24	84.2
6	1.25	0.35	1.46	13.35	33.9
6	1.25	0.45	1.34	13.4	69.5

Table 4 lists the physical and chemical characteristics of the used solutions. It has been established that pH of the alkaline solution plays an important role in the slag dissolution process [45], although this pH value does not directly control the reaction rate. The effect of activator pH on reaction rate of alkali activated slag is at most indirect, as long as the pH is high enough to initiate the dissolution/reaction process [46]. For the particular slag studied in this work, the minimum pH for an effective alkali-activation reaction should be above 10.1 because that is pH measured in a suspension of slag in water with a solution/slag ratio = 0.35.

%Na_2O	**Ms**	**s/s ratio**	**Density (g/cm^3)**	**pH**	**Conductivity (mS)**
4	0.75	0.35	1.23	13.22	164
4	0.75	0.45	1.18	13.24	168
4	1	0.35	1.26	13.66	125.6
4	1	0.375	1.25	13.69	129.6
4	1	0.4	1.22	13.71	131.5
4	1.25	0.35	1.29	13.25	84.9
4	1.25	0.45	1.21	13.38	93.6
4.5	1	0.35	1.3	13.62	112.2
4.5	1	0.375	1.27	13.65	121.1
4.5	1	0.4	1.26	13.68	126.4
5	0.75	0.4	1.26	13.12	156.7
5	1	0.35	1.33	13.54	99.5

5	1	0.375	1.3	13.61	110.4
5	1	0.4	1.3	13.64	117.4
5	1	0.45	1.25	13.33	118.1
5	1.25	0.4	1.31	13.37	76.5
6	0.75	0.35	1.38	12.8	102.7
6	0.75	0.45	1.28	13.23	151.6
6	1	0.4	1.36	13.24	84.2
6	1.25	0.35	1.46	13.35	33.9
6	1.25	0.45	1.34	13.4	69.5

Table 4. Physical and chemical characteristics of the waterglass solutions

2.2 Experimental plan

Alkali activation efficiency has been studied taking into account the influence of following mix design parameters: $\%Na_2O$, Ms and s/s ratio. No additives have been used in this work and all specimens have been cured in a humid chamber with a 100% of relative humidity (HR) and 20 ±2 ºC, except specimens selected for shrinkage tests, for which a 50 ±5% RH was used.

Statistical experimental design methodology has been implemented in the selection of the samples to be prepared in the experimental domain covered by present research, and analysis via response surface curves has been also applied when possible. Response surface analysis includes choosing a proper model for a collected experimental data set and testing the adequacy of the chosen model. This research has been conducted in two stages: first one has a wider experimental domain which consist of three-level, three variable composite experimental design which follows 2^{nd} degree polynomial model; the second stage has focused on a selected area of the first stage experimental domain which demonstrated a better response, and consist of three-level, two variable composite experimental design also following 2^{nd} degree polynomial model. In the first stage study, independent variables are $x_1 = \%Na_2O$, x_2 = s/s ratio and x_3 = Ms. The selected experimental domain, based on bibliographic data [38], has been chosen to achieve a stable activation of the slag. The full quadratic model for three independent variables which has ten coefficients b_0, …, b_9 may be represented with Equation 1. Table 5 shows the experiments selected for the composite experimental design of first stage. Figure 1 depicts the isovariance curves in three cross-sections of the experimental domain. As the experimental domain of first stage study has cubic symmetry a clear idea of the variance in the whole experimental domain can be deduced. In the second stage approach, independent

variables are x_1 = %Na_2O and x_2 = s/s ratio. The full quadratic model for two independent variables which has six coefficients c_0, …, c_5 may be represented with Equation 2. Table 6 shows the experiments selected for the composite experimental design of second stage and Figure 2 the isovariance curves of the experimental domain. In the second stage, the Ms was removed as variable since in the first stage it was deduced that its influence on the selected properties was clearly established and was negligible respect to the other ones. For that reason, an Ms = 1.00 was used in the second stage study.

$$Y = b_0 + b_1 * X_1 + b_2 * X_2 + b_3 * X_3 + b_4 * (X_1*X_1) + b_5 * (X_2*X_2) + b_6 * (X_3*X_3) + b_7 * (X_1*X_2) + b_8 * *(X_1*X_3) + b_9 * (X_2*X_3) \quad \textbf{Eq. 1}$$

$$Y = c_0 + c_1 * X_1 + c_2 * X_2 + c_3 * (X_1*X_1) + c_4 * (X_2*X_2) + c_5 * (X_1*X_2) \quad \textbf{Eq. 2}$$

%Na_2O	4.0	4.0	4.0	4.0	4.0	5.0	5.0	5.0	5.0	5.0	6.0	6.0	6.0	6.0	6.0
Ms	0.75	0.75	1.00	1.25	1.25	0.75	1.00	1.00	1.00	1.25	0.75	0.75	1.00	1.25	1.25
s/s ratio	0.35	0.45	0.40	0.35	0.45	0.40	0.35	0.40	0.45	0.40	0.45	0.35	0.40	0.35	0.45

Table 5. Dosages implemented in the first stage (extended experimental domain) of the experimental plan.

%Na_2O	4.0	4.0	4.0	4.5	4.5	4.5	5.0	5.0	5.0
Ms	1.00	1.00	1.00	1.00	1.00	1.00	1.00	1.00	1.00
s/s ratio	0.35	0.375	0.40	0.35	0.375	0.40	0.35	0.375	0.40

Table 6. Dosages implemented in the second stage (reduced experimental domain) of the experimental plan.

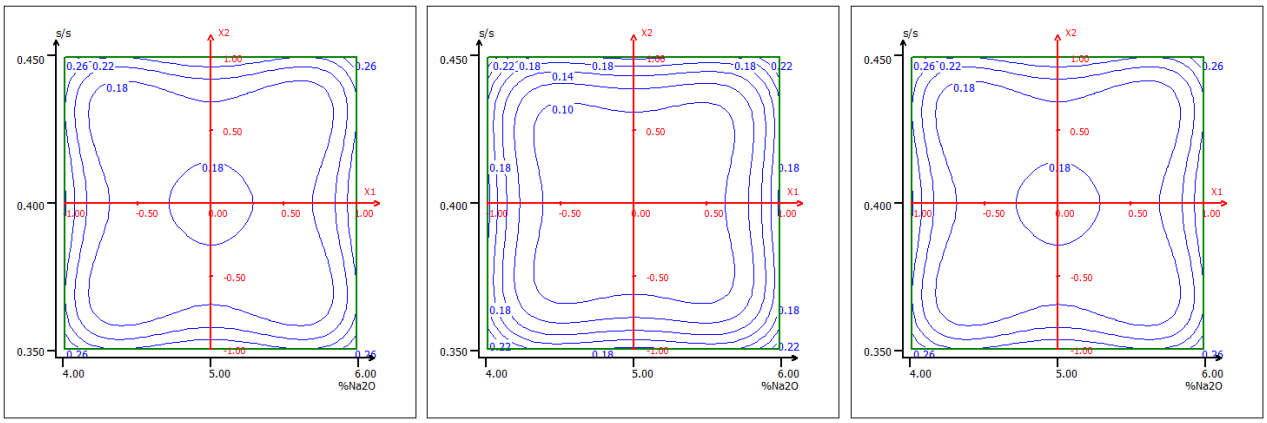

Figure 1. Isovariance curves in the experimental domain of the first stage study for Ms = 0.75 (left), 1.00 (center) and 1.25 (right).

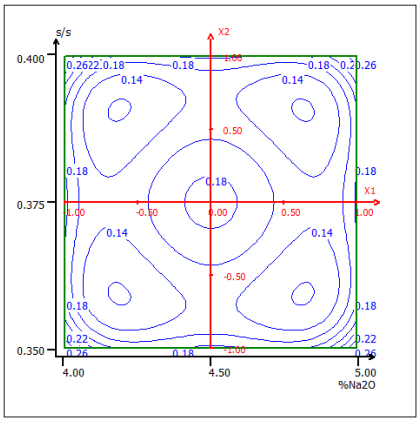

Figure 2. Isovariance curves in the experimental domain of the second stage study for Ms = 1.00.

Two properties were measured on alkali activated SiMn slag pastes prepared in the first stage: fluidity of fresh pastes and compressive strength at 7, 28 and 90 days of curing time. The results obtained in this stage were analysed and then the experimental domain of stage two was proposed. In order to give a better characterization of the most interesting dosages, the following properties were determined for pastes prepared in this second stage of the experimental plan: fluidity of fresh pastes, setting time, compressive strength and shrinkage in a 50% RH environment.

2.3 Sample preparation and tests

The pastes were prepared with 1800 g of SiMn slag and the alkaline solutions listed in Table 5 and Table 6. The pastes were prepared in a mixer Controls Automix, model 65-L0006/A for 3 min according to UNE EN 196-3 [47].

Paste Fluidity (minislump test): Paste fluidity was determined with the minislump test which is a modification of the proposed by Kantro [48]. After mixing the pastes were placed on a flow table in a truncated conical mould measuring 19x38x57 mm. The mould was subsequently removed and the paste was dropped ten times on the flow table. The paste diameter was measured in four directions and the arithmetic mean taken as the final value.

Setting Times: Setting times were determined according to UNE EN 196-3 [47]. These tests have been carried out with a Controls Vicamatic, model 63-L0027/E.

Compressive strength: Three 4 × 4 × 4 cm specimens for each mix given in the experimental work plan (Tables 5 and 6) were fabricated to test compressive strength. The samples were cured in 100% HR for 7, 28

and 90 days at 20 ±2 °C and then tested using a hydraulic press following the standard EN 196-1 [49]. Each compressive strength value was obtained from the average value of the three tests.

Shrinkage: Shrinkage of hardened pastes was tested following the Spanish standard UNE 80112 [50]. Two prismatic paste specimens measuring 285x25x25 mm were prepared for each mix given in the experimental work plan (Table 6). The presented results are the average value of two specimens.

Mercury intrusion porosimetry: Porosity characterization of the pastes was carried out by mercury intrusion porosimetry technique. Both the total connected porosity and the pore size distribution in the 0.0035–250 μm diameter range were obtained. An Autopore IV 9500 Micromeritics mercury porosimeter was used. The Hg pressure interval was 0.5–33,000 psi (0.015–205 MPa).

Scanning Electronic Microscopy: HITACHI S3000N SEM equipped with an energy dispersive X-ray (EDX) Bruker XFlash 3001 was used for microanalysis of pastes.

3. RESULTS AND DISCUSSION

3.1 First stage: extended experimental domain

Paste Fluidity (minislump test)

Figure 3 shows response surface curves for obtained paste fluidity in minislump test for pastes with different Ms values. It can be observed that paste fluidity depends on the $\%Na_2O$ and Ms, as it has been established by other authors in studies about alkali activation of slags with similar composition to the one under investigation in present research [29]. Firstly, as it should be expected, it can be appreciated that fluidity increases as the s/s ratio is increased. On the other hand, for a fixed s/s ratio and Ms, the obtained slump decreases as the $\%Na_2O$ increases, so pastes lose workability. In addition, for a fixed $\%Na_2O$ and s/s ratio, paste slump increases as Ms increases. This observation is more evident for pastes with lower workability, i.e. pastes with low s/s ratio and high $\%Na_2O$.

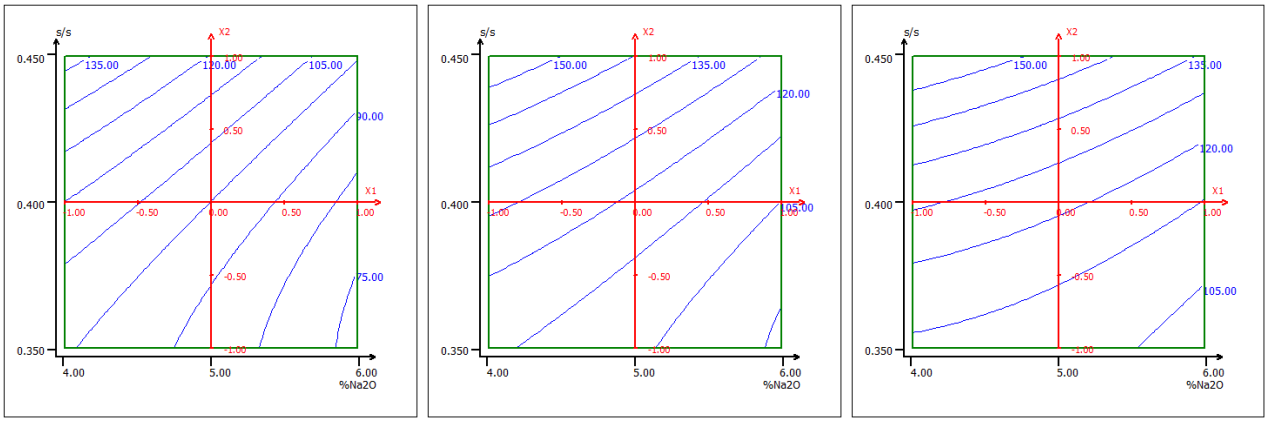

Figure 3. Response surface curves for slump values (in mm) obtained in minislump test for pastes with Ms = 0.75 (left), 1.00 (center) and 1.25 (right).

Compressive strength

Previously to expose compressive strength results obtained for pastes prepared in the extended experimental domain, attention should be paid to the isovariance curves that are applicable to this particular case. Due to the extremely fast setting observed for paste prepared with a 6% of Na_2O, s/s ratio= 0.35 and Ms = 0.75, it was impossible to cast that sample into the mould and the experimental point associated to that sample had to be removed from the experimental design. This circumstance modified the variance of the experimental domain, especially in the area surrounding that experimental point. Figure 4 shows the isovariance curves in three cross-sections of the experimental domain for the compressive strength of alkali activated SiMn pastes. It can be observed the alteration of the variance around the coordinates (6% Na_2O, s/s ratio = 0.35, Ms = 0.75). For that reason, response surface of the compressive strength results of that particular area will have a higher degree of uncertainty, although its significance is relatively low since that area would be affected by fast setting and, in a practical sense, it should be avoided for real applications.

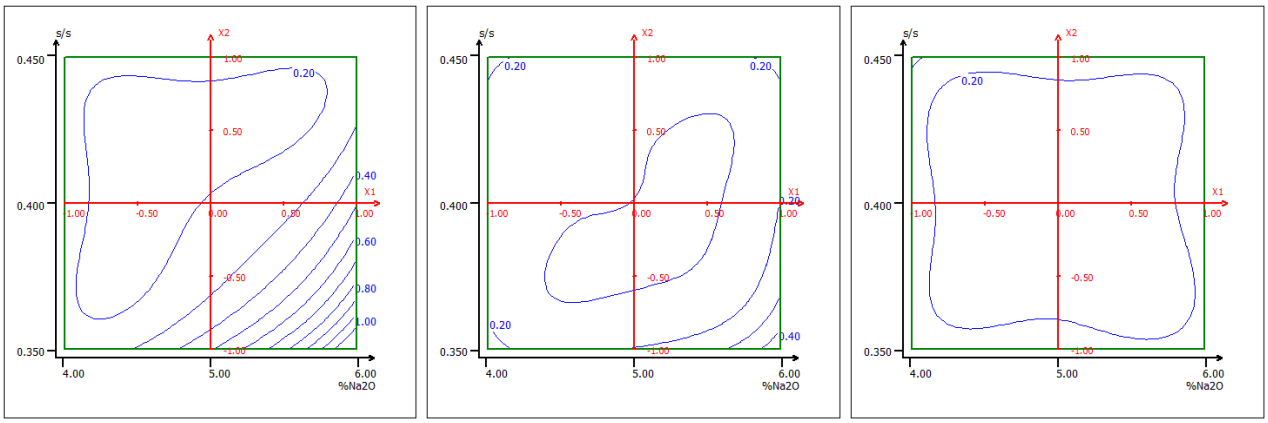

Figure 4. Isovariance curves for the particular case of compressive strength tests of first stage samples. Ms = 0.75 (left), 1.00 (center) and 1.25 (right).

Figure 5 depicts response surface curves for compressive strength values at 7, 28 and 90 days of curing time for pastes with Ms = 0.75, 1.00 and 1.25. Firstly, it can be observed a positive evolution of compressive strength over time, which highlights the limited reactivity of this slag in the short term as it has been established by other authors [7]. According to them, manganese seems to have a negative influence on the reactivity and strength of SiMn slag at early age, but it does not hinder long-term activation. The best performance at 90 days of curing time offered compressive strength values higher than 35 MPa.

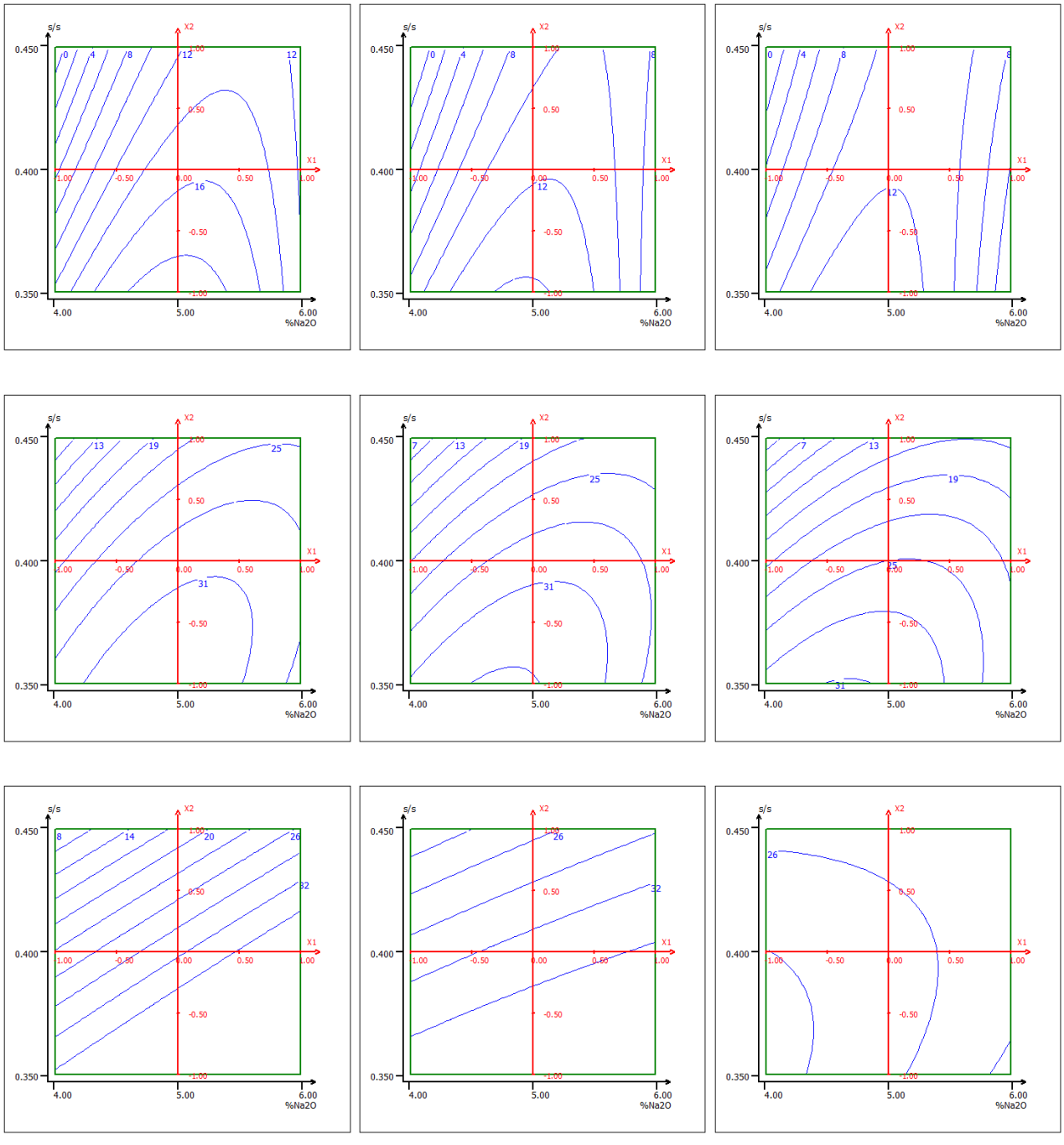

Figure 5. Response surface curves for compressive strength values (in MPa) at 7 days (top row), 28 days (center row) and 90 days (bottom row) of curing time of pastes with Ms = 0.75 (left column), 1.00 (center column) and 1.25 (right column).

Additionally, it can be observed that for a fixed $\%Na_2O$ and s/s ratio, when a Ms value higher that 1.00 is adopted, a decrease in mechanical strength is registered. This behaviour can be explained by the impact that the competence between initiation step of alkaline activation (dissolution process) and C-S-H gel formation has on mechanical strength [38]. If activation conditions favours C-S-H formation due to a high Ms, but the activation is hindered by a low $\%Na_2O$, the result is a decrease in compressive strength. On the contrary, if $\%Na_2O$ is high enough to promote good activation conditions, the increase in SiO_2 content will result in a higher formation of gels and an increase in mechanical strength. The obtained results in present research agree with other authors who indicate that an optimal range of Ms values exists for any particular $\%Na_2O$ in the activator. These conditions combine high enough OH^- concentration to dissolve the slag and high enough SiO_2 content to enhance C-S-H gel formation and precipitation [29]. In addition, it can be observed that at 7 days of curing time, higher compressive strength is obtained as Ms decreases, which is in accordance with other authors' results [33]. However, at 28 and 90 days of curing time, compressive strength increases as Ms is increased up to a value from which decreases. The optimal Ms value found in this research for the activation of SiMn slag is around 1.00, which agrees with the optimal range stated in other works (0.75-1.25) for similar acid slags [38].

For fixed $\%Na_2O$ and Ms values, it can be observed that, in general, the higher the s/s ratio the lower the mechanical strength is registered. This behaviour can be related to the total porosity that should be expected when s/s ratio is increased since, this type of binders do not have the benefit of converting water into a solid form and thereby reducing pore volume. In geopolymer binders the absolute pore volume is not affected by the formation of hydration products and there is no water bound into the solidified geopolymer gel [44]. This statement is validated by the following data: total porosity of pastes prepared with Ms = 1.00 and 4.5% Na_2O is 19.7% for s/s ratio = 0.35, and 23.4% for s/s ratio = 0.40; and they agree with the higher mechanical strength obtained at lower s/s ratio in spite of the lower workability. On the other hand, it can be observed that this dependence is very evident at low $\%Na_2O$ (small variations on s/s ratio strongly affect compressive strength) and is not so pronounced at higher $\%Na_2O$.

It can be observed that SiMn slag activated with waterglass is very sensitive to $\%Na_2O$ in the activating solution. At 7 and 28 days of curing time, compressive strength increases when $\%Na_2O$ is increased up to a certain concentration range in which the compressive strength remains approximately constant, and then, if $\%Na_2O$ surpasses that concentration range, a decrease in the strength is registered. Thus, for any Ms value within the studied range, a zone in the centre of the experimental domain can be appreciated which exhibits the highest mechanical strength, outside which their values decrease. At 28 days of curing time, the $\%Na_2O$ range in which the highest compressive strength is obtained has been extended at the expense of a higher influence of s/s ratio, that is to say that isolevel lines are more perpendicular to s/s axis. This result agrees to other researchers' findings [38] which established the existence of an optimal $\%Na_2O$ that lays between 3.0-5.5% Na_2O. At 90 days of curing time, for Ms lower than 1.00 the behaviour is similar to that one observed at 7 and 28 days, taking into account the zone near to Ms = 0.75, s/s ratio = 0.35 and 6% Na_2O, because that experimental points has been removed due to the abovementioned reasons. For Ms higher than 1.00, both s/s ratio and $\%Na_2O$ exhibit lower influence in compressive strength since isolevel lines are more separated from each other.

On the other hand, it is also observed a clear interrelation between $\%Na_2O$ and s/s ratio, in the way that if $\%Na_2O$ is increased, it is advisable to also increase s/s ratio, but up to certain value from which mechanical strength will decrease. Other authors [38] have established the existence of an optimal value for s/s ratio and if that point is exceeded, the strength would be reduced. Their explanation is based on the opposing effect produced by the increase of the alkaline component responsible of enhancing the activation which increases mechanical strength, and the increase of the pore volume in the hardened paste which reduces mechanical strength. For low s/s ratio, the phenomenon is directed by the positive effect of the alkaline activation, so the mechanical strength is increased. For intermediate s/s values, both processes reach an equilibrium. And for high s/s ratios, increment in the pore volume is the leading factor, thus compressive strength decreases. Results of present work agree at 7 and 28 days with that behaviour, but that optimal s/s value has not been detected at 90 days, which could be due to the development of the polymerization process which compensates the higher porosity of pastes prepared with high s/s ratio. In this case, it is observed that Ms exerts a clear influence in the values and behaviour of the rest of parameters under analysis. Therefore, for Ms values similar or lower to 1.00 a direct relationship between $\%Na_2O$ and s/s ratio with compressive

strength is observed at 90 days of curing time, so to obtain a particular strength, increasing %Na_2O implies to increase s/s, although this relationship is less pronounced when Ms increases.

Compressive strength values higher than 10-12 MPa have been calculated for a wide range of conditions around 5% Na_2O, at 7 days of curing time. The maximum compressive strength at early age has been higher than 12 MPa, and has been obtained on pastes with s/s ratio lower than 0.40 and around 5% Na_2O. At 28 days of curing time, the intermediate Ms shows the best compromise since it offers compressive strength values higher than 30 MPa in a wide %Na_2O range for s/s ratios lower than 0.40. The best performance was obtained for pastes with s/s ratio lower than 0.40, 4.0-5.5% Na_2O and Ms similar or lower than 1, which offered compressive strength values around 31 MPa. Finally, at 90 days, compressive strength values higher than 35 MPa were obtained for pastes with s/s ratio lower than 0.40 and 5.0-6.0% Na_2O for Ms = 1.00, and 4.0-5.0% Na_2O for Ms = 0.75. It has been taken into account the high statistical uncertainty in the region near to 6% Na_2O and s/s = 0.35 due to the removal of that particular point in the experimental design for fast setting problems, which recommends to avoid that dosage zone. For Ms higher than 1.00, the behaviour is different; lower mechanical strength is obtained and lower influence of mix design parameter (s/s ratio and %Na_2O) are observed, although compressive strength up to 29 MPa can be achieved for s/s ratio lower than 0.40 and 4.0-4.5% Na_2O.

If the results of this research at 28 days of curing time are compared to those published by Kumar et al. [6] referred to SiMn slag with ball milling activation and using NaOH as activator, it can be observed that mechanical strength obtained with waterglass as activator are higher. In that particular research activating solution consists of 6% Na_2O and 0.35 s/s ratio. It should be noticed that, in present research, %Na_2O is lower (4.0-5.0%) and milling time is also lower (25 min). These results agree with other works which indicate that waterglass is better activator from the mechanical performance point of view, highlighting the important role played by silicate ions in the activating solution [38,45]. It has been established [45] that the pH level of the alkaline solution is a key factor in the slag dissolution process. And for pH values higher than 12, as the ones presented in both studies, the main factor that controls setting time and mechanical strength development is the anion type of the activating solution.

The aforementioned arguments highlight the interdependence of the different factors which act in the activation process, and the relevance of the Na_2O and SiO_2 content as critical parameters in the control of the

mechanical strength developed by alkali-activated SiMn slag with waterglass, as it has been evidenced by other authors in the activation of different waste materials [29,38,51,52].

Taking into account the aforementioned results and with the aim of determining the optimal activation parameters to achieve the best mechanical performance with an adequate workability, a second stage on the experimental work plan was established. The experimental domain was reduced to be focused in the following mix design: 4.0-5.0 %Na_2O, 0.35-0.40 s/s ratio and Ms = 1.00.

3.2 Second stage: reduced experimental domain

As it has been explained before, the results included in this section are obtained in a reduced experimental domain which has been selected considering the analysis made in the first part of the study.

Paste Fluidity (minislump test)

Figure 6 shows response surface curve calculated for slump values of alkali-activated SiMn slag pastes with Ms = 1.00. As it could be expected, for a fixed %Na_2O, the higher the s/s ratio the higher the fluidity observed in the paste. However, as a result of the focus that has been made respect to the original experimental domain analysed in the first stage of this work (Figure 3), it can be noted that for given s/s ratio, the fluidity of paste increases as %Na_2O is increased up to a certain percentage, and then it drops if %Na_2O continues increasing. These results show that around 4.5% Na_2O the fluidity of the paste is maximum.

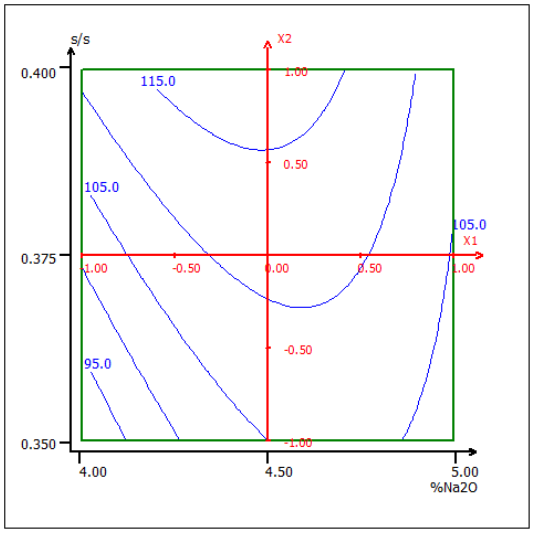

Figure 6. Response surface curve of slump values (in mm) for alkali-activated SiMn slag pastes with Ms = 1.00.

Setting Times

Table 7 shows initial, final setting times as well as workability time (Δt) of alkali-activated SiMn pastes for different s/s ratios and %Na_2O, and Figure 7 depicts response surface curve of workability time, calculated as the difference between final and initial setting times according to UNE 196-3 [47]. It can be observed that for a fixed s/s ratio, workability time decreases for increasing percentages of Na_2O. This results is consistent with fluidity values observed and with results published by other authors who conclude that an increase in the %Na_2O produces an effect on the fluidity reducing workability time [29,33]. In turn, s/s ratio also exhibits an influence on the paste workability time in the sense that the higher the s/s, the longer the workability time that can be obtained. Additionally a maximum workability time can be measured for a given %Na_2O when s/s ratio is increased up to a certain ratio, beyond which the paste offers lower workability time. The longest workability times are achieved for pastes fabricated with s/s ratio between 0.37 and 0.39, and %Na_2O lower than 4.3. Kumar et al. [6] obtained longer setting times due to the activator that was used in that research (NaOH), since setting times are significantly reduced in presence silicate anions, accordingly to the arguments exposed by other authors [45].

s/s	**0.35**			**0.375**			**0.40**		
%Na_2O	**4.0**	**4.5**	**5.0**	**4.0**	**4.5**	**5.0**	**4.0**	**4.5**	**5.0**
Initial setting (min)	46	102	38	71	67	99	263	56	62
Final setting (min)	141	187	81	196	157	179	368	151	137
Δt (min)	95	85	43	125	90	80	105	95	75

Table 7. Setting times of alkali-activated SiMn slag pastes according to UNE 196-3.

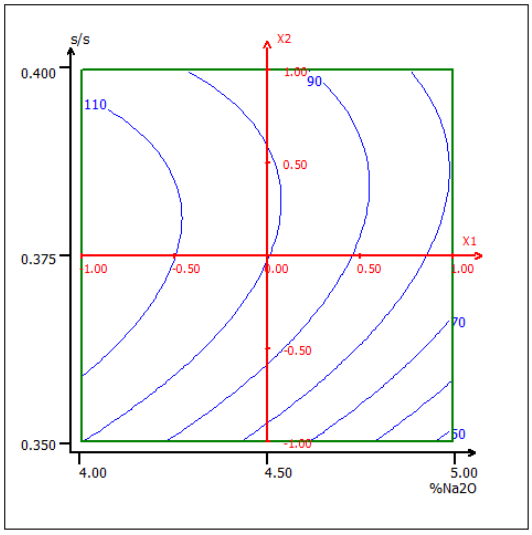

Figure 7. Response surface curve of workability time (Δt = initial setting – final setting) (in min) of pastes with Ms = 1.00 obtained according to UNE 196-3 [47]**.**

Compressive strength

Figure 8 shows response surface curves for compressive strength at different curing times of alkali-activated SiMn slag pastes with Ms = 1.00. Firstly, it can be noticed that obtained values are consistent with those ones shown by first stage experiments (Figure 5). It can be observed that the strength gain for pastes with high s/s ratio and low %Na_2O is rather slow, at early age. However, at 28 and 90 days of curing time, compressive strength is higher than 25 and 35 MPa, respectively, within the proposed experimental domain. With regard to the influence of %Na_2O, it can be noted that highest values are within the 4.3-4.8% range at 7 days of curing time, with a maximum strength of 16 MPa. At 28 days of curing time, the optimal concentration of Na_2O is located in the 4.5-4.7% range, with a highest value around 36 MPa. Finally, after 90 days of curing time, the best compressive strength is obtained around 4.6% Na_2O, offering values higher than 48 MPa for a s/s ratio near to 0.35, in spite of the reduction in workability shown by those samples. As it was mentioned before, for a fixed %Na_2O, the higher the s/s ratio, the higher the total porosity that is measured, and the lower the compressive strength that is observed. This behaviour is because this type of binders do not incorporate water into their geopolymeric structure and thus, forming hydration products contribute to reduce total pore volume and to improve their mechanical performance. Therefore, the quality of the material depends on its water demand [44].

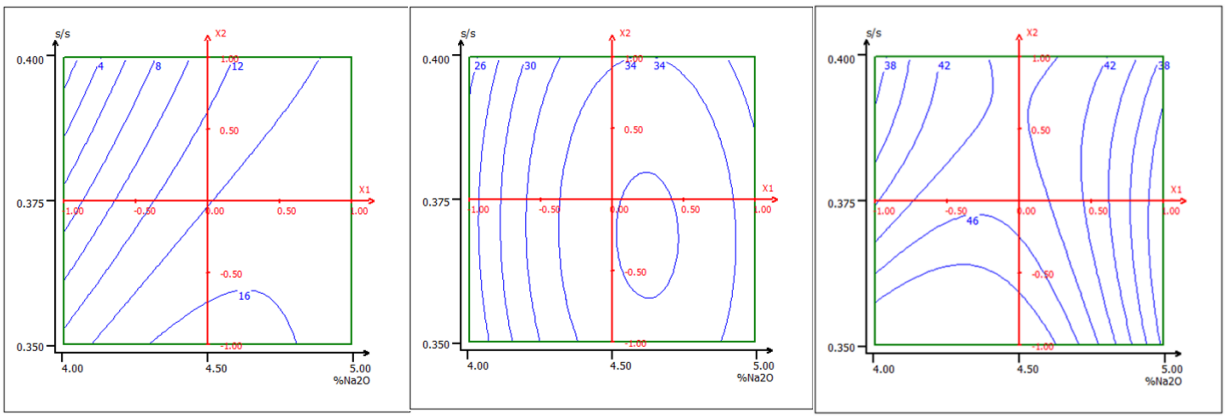

Figure 8. Response surface curves for compressive strength values (in MPa) at 7 days (left), 28 days (center) and 90 days (right) of curing time of pastes with Ms = 1.00.

Shrinkage

Figure 9 shows specimen length evolution of alkali-activated SiMn slag pastes stored at 20±1 ºC and 50±5% RH. The time required by these paste specimens to stabilize their lengths has been 30 days, approximately. In addition, it can be observed that shrinkage is evident for all specimens, which is attributed to the low relative humidity of the ambient where specimens were stored, which was precisely selected to magnify the shrinkage process and show the behaviour of this materials in the worst possible conditions. Further studies of this property in humid chamber are recommended to check the extension of the shrinkage reduction that is expected to occur, like it happens with other alkali-activated materials [53,54]. Additionally, it should be tested the influence of Ms parameter on shrinkage in order to verify if samples prepared with Ms = 1 offer the highest autogenous shrinkage, as other authors suggest [33],

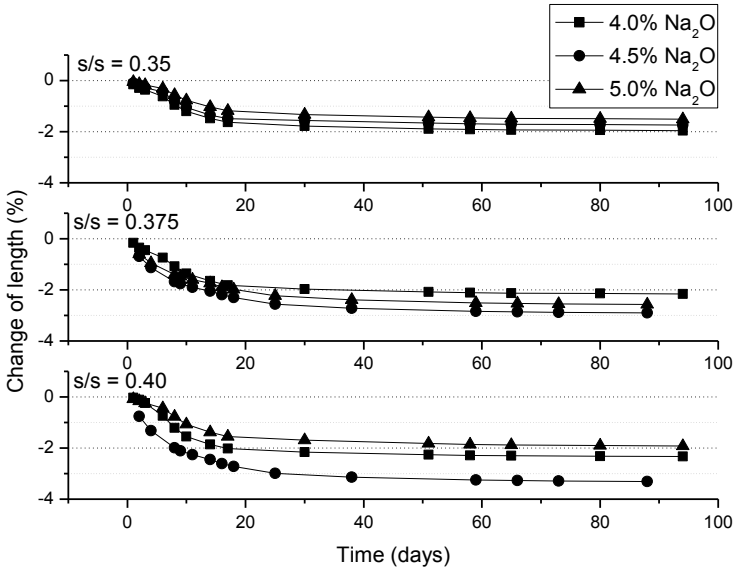

Figure 9. Evolution of length of alkali-activated SiMn slag pastes in a 50% RH ambient.

In order to show a better tool to analyse the influence of mix design parameters on shrinkage, Figure 10 presents response surface curve of shrinkage after 90 days in a 50% RH ambient for alkali-activated SiMn slag pastes with Ms = 1.00. With regard to the evolution of shrinkage for any s/s ratio, a maximum value can be observed at 4.5% Na_2O. Besides, for s/s values under 0.375, the higher the s/s ratio the higher the shrinkage that is registered. Above s/s = 0.375, this tendency is reduced and eventually reversed. Thus, maximum shrinkage is registered for s/s ratio around 0.38 and 4.5% Na_2O for pastes with Ms = 1.00. The behaviour observed in this property is explained by the more refined pore structure that is presented for

samples with higher s/s ratio. Other authors explain the shrinkage observed on alkali-activated slags in terms of their pore structure and C-S-H gel microstructure [55,56].

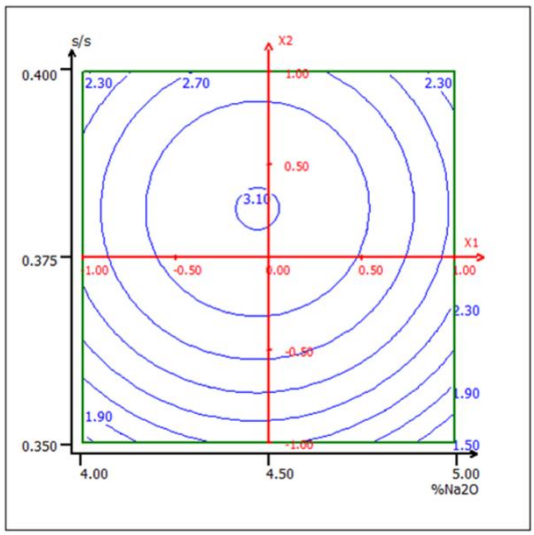

Figure 10. Response surface curve of shrinkage after 90 days in a 50% RH ambient for alkali-activated SiMn slag pastes with Ms = 1.00.

Figure 11 shows pore size distributions of alkali-activated SiMn slag pastes with Ms = 1.00, 4.5% Na_2O and two levels of s/s ratio, after shrinkage test, i.e. stored at 50% RH for 100 days. It can be noted that paste with higher s/s (0.40) presents a more refined pore structure with higher pore volume with diameter under 10 nm, which are mainly responsible of shrinkage phenomenon. It has been established that a higher mesopores content (1.25-25 nm) implies greater capillary stress and thus, higher drying shrinkage [54,57].

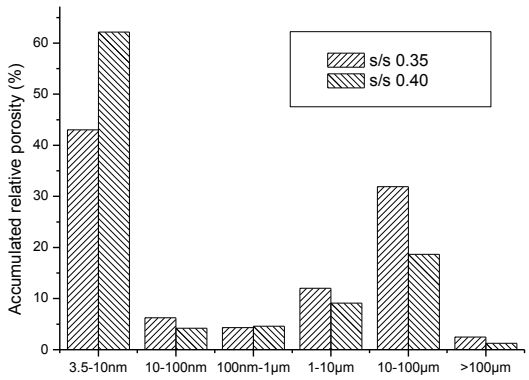

Figure 11. Pore size distributions of alkali-activated SiMn slag pastes with Ms = 1.00 and 4.5% Na_2O, stored at 50% RH for 100 days.

In addition, a microstructural analysis by SEM/EDS has been carried out on these particular samples. Table 8 shows a summary of main elemental ratios from EDS analysis. Those results evidence that there are not

significant differences in the formed C-S-H, and both samples offer similar Ca/Si ratios and their values are consistent with other authors' results for slags with similar composition [58]. This results agrees with the fact that both pastes present similar compressive strength, in spite of showing different shrinkage level. Other authors that have used the same slag but activated with NaOH [6] have obtained similar Ca/Si ratios, higher Al/Si ratios and lower Ca/Mn, thus it may be deduced that activation with waterglass yields a lower incorporation of Al and Mn content in the structure.

Paste	**Ca/Si**	**Na/Si**	**Al/Si**	**Ca/Mn**
4.5% Na_2O – s/s 0.35 – Ms = 1.00	1.35	0.39	0.31	2.63
4.5% Na_2O – s/s 0.40 – Ms = 1.00	1.44	0.38	0.30	3.16

Table 8. Summary of main elemental ratios from EDS analysis.

Calculated coefficients of the model

Finally, this section summarizes the calculated coefficients of the proposed model that has been implemented in this work. Table 9 and Table 10 present the coefficients for model applied in first stage experiments and second stage experiments, respectively. Information between parentheses in those tables do not refer to the units of the coefficients but the units resulting in the application of coefficients in each model equation. Prior to use those coefficients it must be considered that independent variables (x_1 to x_n) of each model has to be included as non-dimensional and normalized units in the range from -1 to +1, which represent the minimum and maximum value of the experimental domain of each variable. For example, the quantity of Na_2O investigated in first section experiments ranges from 4.0 to 6.0 %Na_2O so the following equation $x_1 = \%Na_2O - 5$ must be used to convert real values of variables into non-dimensional and normalized units.

Coefficient	**Fluidity (mm)**	**Compressive strength (MPa)**		
		7 days	**28 days**	**90 days**
$\mathbf{b_0}$	118.5	11.61	29.6	33.9
$\mathbf{b_1}$	-12.4	2.17	2.8	1.1
$\mathbf{b_2}$	18	-2.73	-7.4	-5.1
$\mathbf{b_3}$	12.2	-1.97	-2.5	-0.7
$\mathbf{b_4}$	-1.33	-6.69	-5.1	-1.3
$\mathbf{b_5}$	5.79	0.15	-2.7	-2.3
$\mathbf{b_6}$	-8.9	1.98	-2.2	-4.8

b_7	-3.65	3.04	4.8	3.3
b_8	4.06	-1.38	-1.3	-3.3
b_9	1.67	1.38	-1	3.8

Table 9. Calculated coefficients of the proposed model (Equation 1) for the first stage of the study (extended experimental domain).

Coefficient	Fluidity (mm)	Workability time (Δt) (min)	Compressive strength (MPa)			Shrinkage (%)
			7 days	28 days	90 days	
c_0	111.5	119.1	13.9	35.9	45.1	3.06
c_1	1.94	-27	3.72	2.8	-3.8	-0.08
c_2	6.28	15.3	-3	-0.7	-3.1	0.32
c_3	-8.83	-8.7	-3.5	-5.9	-7.1	-0.57
c_4	-0.24	-23.7	0	-1.4	2.4	-0.62
c_5	-4.44	5.5	3	-0.3	4.2	0.01

Table 10. Calculated coefficients of the proposed model (Equation 2) for the second stage of the study (reduced experimental domain).

4. CONCLUSIONS

Alkali activation procedure has been successfully applied to SiMn slag for pastes preparation using waterglass as alkaline activator. Statistical experimental design methodology has been used to study the influence of $\%Na_2O$, Ms and s/s ratio in workability, setting time, compressive strength and shrinkage. Response surface analysis and a proper model for a collected experimental data set were done. The following are the key conclusions:

1. The paste fluidity depends on the $\%Na_2O$ and Ms. For a given s/s ratio, the fluidity of paste increases as $\%Na_2O$ is increased up to a certain percentage, and then it drops if $\%Na_2O$ continues increasing. For a fixed s/s ratio, workability time decrease for increasing percentages of Na_2O. A maximum workability time can be measured for a given $\%Na_2O$ when s/s ratio is increased up to a certain ratio, beyond which the paste offers lower workability time. An optimal range of Ms values exists for any particular $\%Na_2O$ in the activator. It has been shown the relevance of the Na_2O and SiO_2 content as critical parameters in the control of the mechanical strength developed by alkali-activated SiMn slag with waterglass.
2. If workability, setting time and compressive strength are considered as main properties, an optimal dosage can be proposed according to the following parameters: Ms = 1.00, 4.5 $\%Na_2O$ and s/s ratio lower than 0.375. With these conditions, a compressive strength of 46 MPa has been achieved at 90 days of

curing time. However, for any s/s ratio, a maximum value of shrinkage can be observed at 4.5% Na_2O. The analysed properties have been modelled by equations that can be applied within the experimental domain explored in this research.

3. High shrinkage values have been registered for all pastes in the 50% RH ambient. In these conditions, shrinkage achieves a stable value after 30 days. Shrinkage levels have ranged from 1.5% to 3.0% approximately and its maximum value is observed for s/s ratio around 0.38 and 4.5% Na_2O in pastes with Ms = 1.00.
4. The results obtained show that it is possible to valorise the SiMn slag through its use as an alkali activated binder.

ACKNOWLEDGEMENT

The authors wish to thank the Spanish Ministry of Economy and Competitiveness and European Union (FEDER) for project funding (BIA 2014-58194-R). The authors also wish to thank Cristina Rodríguez from Ferroatlántica, S.A., for the supply of SiMn slag necessary to carry out this research.

REFERENCES

[1] C. Shi, A.F. Jiménez, A. Palomo, New cements for the 21st century: The pursuit of an alternative to Portland cement, Cem. Concr. Res. 41 (2011) 750–763. doi:10.1016/j.cemconres.2011.03.016.
[2] M.C.G. Juenger, F. Winnefeld, J.L. Provis, J.H. Ideker, Advances in alternative cementitious binders, Cem. Concr. Res. 41 (2011) 1232–1243. doi:10.1016/j.cemconres.2010.11.012.
[3] K.H. Yang, Y.B. Jung, M.S. Cho, S.H. Tae, Effect of supplementary cementitious materials on reduction of CO2 emissions from concrete, J. Clean. Prod. 103 (2015) 774–783. doi:10.1016/j.jclepro.2014.03.018.
[4] J. Vargas, A. Halog, Effective carbon emission reductions from using upgraded fly ash in the cement industry, J. Clean. Prod. 103 (2015) 948–959. doi:10.1016/j.jclepro.2015.04.136.
[5] Essential Manganese, Int. Manganese Inst. (2016). http://www.manganese.org/images/uploads/publications/97_16_REPORT-BAT-1.pdf (accessed May 26, 2017).
[6] S. Kumar, P. García-Triñanes, A. Teixeira-Pinto, M. Bao, Development of alkali activated cement from mechanically activated silico-manganese (SiMn) slag, Cem. Concr. Compos. 40 (2013) 7–13. doi:10.1016/j.cemconcomp.2013.03.026.
[7] J. Péra, J. Ambroise, M. Chabannet, Properties of blast-furnace slags containing high amounts of manganese, Cem. Concr. Res. 29 (1999) 171–177. doi:10.1016/S0008-8846(98)00096-9.
[8] M. Frías, M.I. Sánchez de Rojas, O. Rodríguez, C. Rodríguez, Valorización de la escoria de SiMn como material puzolánico para la fabricación de cementos, Cemento-Hormigón. (2009) 18–25.
[9] M. Frias, M.I. Sánchez de Rojas, J. Santamaría, C. Rodríguez, Recycling of silicomanganese slag as pozzolanic material in Portland cements: Basic and engineering properties, Cem. Concr. Res. 36 (2006) 487–491. doi:10.1016/j.cemconres.2005.06.014.
[10] M. Frías, M.I.S. de Rojas, C. Rodríguez, The influence of SiMn slag on chemical resistance of

blended cement pastes, Constr. Build. Mater. 23 (2009) 1472–1475. doi:10.1016/j.conbuildmat.2008.06.012.
[11] M. Frías, C. Rodríguez, Effect of incorporating ferroalloy industry wastes as complementary cementing materials on the properties of blended cement matrices, Cem. Concr. Compos. 30 (2008) 212–219. doi:10.1016/j.cemconcomp.2007.05.004.
[12] A. Rai, J. Prabakar, C.B. Raju, R.K. Morchalle, Metallurgical slag as a component in blended cement, Constr. Build. Mater. 16 (2002) 489–494. doi:10.1016/S0950-0618(02)00046-6.
[13] A. Allahverdi, S. Ahmadnezhad, Mechanical activation of silicomanganese slag and its influence on the properties of Portland slag cement, Powder Technol. 251 (2014) 41–51. doi:10.1016/j.powtec.2013.10.023.
[14] S. Choi, J. Kim, S. Oh, D. Han, Hydro-thermal reaction according to the CaO/SiO2 mole-ratio in silico-manganese slag, J. Mater. Cycles Waste Manag. (2015). doi:10.1007/s10163-015-0431-6.
[15] H. Kuhl, The influence of the fine particle structure on the strength properties of Portland cement, Zement. 19 (1930) 60–78.
[16] A.O. Purdon, The action of alkalis on blast-furnace slag, J. Soc. Chem. Ind. 59 (1940) 191–202.
[17] V.D. Glukhovsky, Soil Silicate Articles and Structures, in: Budivelnyk Publisher, Kiev, 1967: p. 156.
[18] M. Schneider, M. Romer, M. Tschudin, H. Bolio, Sustainable cement production-present and future, Cem. Concr. Res. 41 (2011) 642–650. doi:10.1016/j.cemconres.2011.03.019.
[19] B. Lothenbach, K. Scrivener, R.D. Hooton, Supplementary cementitious materials, Cem. Concr. Res. 41 (2011) 1244–1256. doi:10.1016/j.cemconres.2010.12.001.
[20] J.S.J. Van Deventer, J.L. Provis, P. Duxson, Technical and commercial progress in the adoption of geopolymer cement, Miner. Eng. 29 (2012) 89–104. doi:10.1016/j.mineng.2011.09.009.
[21] P. Duxson, J.L. Provis, G.C. Lukey, J.S.J. van Deventer, The role of inorganic polymer technology in the development of "green concrete," Cem. Concr. Res. 37 (2007) 1590–1597. doi:10.1016/j.cemconres.2007.08.018.
[22] a Mellado, C. Catalán, N. Bouzón, M. V Borrachero, J.M. Monzó, J. Payá, Carbon footprint of geopolymeric mortar: Study of the contribution of the alkaline activating solution and assessment of an alternative route, RSC Adv. 4 (2014) 23846–23852. doi:10.1039/c4ra03375b.
[23] L.K. Turner, F.G. Collins, Carbon dioxide equivalent (CO2-e) emissions: A comparison between geopolymer and OPC cement concrete, Constr. Build. Mater. 43 (2013) 125–130. doi:10.1016/j.conbuildmat.2013.01.023.
[24] B.C. McLellan, R.P. Williams, J. Lay, A. Van Riessen, G.D. Corder, Costs and carbon emissions for geopolymer pastes in comparison to ordinary portland cement, J. Clean. Prod. 19 (2011) 1080–1090. doi:10.1016/j.jclepro.2011.02.010.
[25] A. Palomo, M.W. Grutzeck, M.T. Blanco, Alkali-activated fly ashes: A cement for the future, Cem. Concr. Res. 29 (1999) 1323–1329. doi:10.1016/S0008-8846(98)00243-9.
[26] A. Fernández-Jiménez, A. Palomo, C. López-Hombrados, Engineering properties of alkali activated fly ash concrete, ACI Mater. J. 103 (2006) 106–112.
[27] E. Douglas, A. Bilodeau, V.M. Malhotra, Properties and durability of alkali activated slag concrete, ACI Mater. J. 89 (1992) 509–516.
[28] A. Fernandez-Jimenez, I. García-Lodeiro, A. Palomo, Durability of alkali-activated fly ash cementitious materials, J. Mater. Sci. 42 (2007) 3055–3065. doi:10.1007/s10853-006-0584-8.
[29] F. Puertas, C. Varga, M.M. Alonso, Rheology of alkali-activated slag pastes. Effect of the nature and concentration of the activating solution, Cem. Concr. Compos. 53 (2014) 279–288. doi:10.1016/j.cemconcomp.2014.07.012.
[30] P. Duxson, A. Fernández-Jiménez, J.L. Provis, G.C. Lukey, A. Palomo, J.S.J. Van Deventer, Geopolymer technology: The current state of the art, J. Mater. Sci. 42 (2007) 2917–2933.
[31] J.L. Provis, A. Palomo, C. Shi, Advances in understanding alkali-activated materials, Cem. Concr. Res. 78 (2015) 110–125. doi:10.1016/j.cemconres.2015.04.013.
[32] S. Kumar, R. Kumar, S.P. Mehrotra, Influence of granulated blast furnace slag on the reaction, structure and properties of fly ash based geopolymer, J. Mater. Sci. 45 (2010) 607–615. doi:10.1007/s10853-009-3934-5.
[33] T. Bakharev, J.G. Sanjayan, Y.B. Cheng, Alkali activation of Australian slag cements, Cem. Concr. Res. 29 (1999) 113–120. doi:10.1016/S0008-8846(98)00170-7.
[34] A. Fernández-Jiménez, F. Puertas, I. Sobrados, J. Sanz, Structure of calcium silicate hydrates formed in alkaline-activated slag: Influence of the type of alkaline activator, J. Am. Ceram. Soc. 86 (2003) 1389–1394. http://www.scopus.com/inward/record.url?eid=2-s2.0-

0043009770&partnerID=tZOtx3y1.
[35] S. Aydın, A ternary optimisation of mineral additives of alkali activated cement mortars, Constr. Build. Mater. 43 (2013) 131–138. doi:10.1016/j.conbuildmat.2013.02.005.
[36] G.E.. Box, K. Wilson, On the experimental attainment of optimum conditions, JR Stat Soc Ser B. 13 (1951) 1–45.
[37] F. Puertas, Escorias de alto horno : composición y comportamiento hidráulico, Mater. Construcción. 43 (1993) 37–48. doi:10.3989/mc.1993.v43.i229.687.
[38] S.D. Wang, K.L. Scrivener, P.L. Pratt, Factors affecting the strength of alkali-activated slag, Cem. Concr. Res. 24 (1994) 1033–1043. doi:10.1016/0008-8846(94)90026-4.
[39] A.G. De La Torre, S. Bruque, M.A.G. Aranda, Rietveld quantitative amorphous content analysis, J. Appl. Crystallogr. 34 (2001). doi:10.1107/S0021889801002485.
[40] UNE 80225:2012. Methods of testing cement. Chemical analysis. Determination of reactive SiO2 content in cements, puzzolanas and fly ash., (2012).
[41] UNE 196-2:2014. Method of testing cement. Part 2: Chemical analysis of cement., (2014).
[42] F. Pacheco-Torgal, J. Castro-Gomes, S. Jalali, Alkali-activated binders: A review. Part 2. About materials and binders manufacture, Constr. Build. Mater. 22 (2008) 1315–1322. doi:10.1016/j.conbuildmat.2007.03.019.
[43] UNE EN 196-6:2010 Methods of testing cement. Part 6: Determination of fineness, (2010).
[44] J.L. Provis, P. Duxson, J.S.J. van Deventer, The role of particle technology in developing sustainable construction materials, Adv. Powder Technol. 21 (2010) 2–7. doi:10.1016/j.apt.2009.10.006.
[45] A. Fernandez-Jimenez, F. Puertas, Effect of activator mix on the hydration and strength behaviour of alkali-activated slag cements, Adv. Cem. Res. 15 (2003) 129–136. doi:10.1680/adcr.15.3.129.36623.
[46] A. Kashani, J.L. Provis, G.G. Qiao, J.S.J. Van Deventer, The interrelationship between surface chemistry and rheology in alkali activated slag paste, Constr. Build. Mater. 65 (2014) 583–591. doi:10.1016/j.conbuildmat.2014.04.127.
[47] UNE EN 193-3:2005+A1:2008. Methods of testing cement. Part 3: Determination of setting times and soundness, (2005).
[48] D.L. Kantro, Influence of Water-Reducing Admixtures on Properties of Cement Paste - A Miniature Slump Test, Cem. Concr. Aggregates. 2 (1980) 95–102. doi:http://dx.doi.org/10.1520/CCA10190J. ISSN 0149-6123.
[49] EN 196-1:2005. Methods of testing cement. Part 1: determination of strength, (2005).
[50] UNE 80112:2016 Test methods of cements. Physical analysis. Determination of contraction in air and expansion in water, (2016).
[51] A. Fernández-Jiménez, A. Palomo, Composition and microstructure of alkali activated fly ash binder: Effect of the activator, Cem. Concr. Res. 35 (2005) 1984–1992. doi:10.1016/j.cemconres.2005.03.003.
[52] A. Fernández-Jiménez, J.G. Palomo, F. Puertas, Alkali-activated slag mortars: Mechanical strength behaviour, Cem. Concr. Res. 29 (1999) 1313–1321. doi:10.1016/S0008-8846(99)00154-4.
[53] F. Collins, J.G. Sanjayan, Strength and shrinkage properties of alkali-activated slag concrete placed into a large column, Cem. Concr. Res. 29 (1999) 659–666. doi:10.1016/S0008-8846(99)00011-3.
[54] M. Palacios, F. Puertas, Effect of shrinkage-reducing admixtures on the properties of alkali-activated slag mortars and pastes, Cem. Concr. Res. 37 (2007) 691–702. doi:10.1016/j.cemconres.2006.11.021.
[55] F.. Wittmann, Creep and shrinkage mechanisms, in: Z.P. Bazant, F.H. Wittmann (Eds.), Creep Shrinkage Concr. Struct., Wiley, Chichester., 1982: pp. 129–161.
[56] J.F. Young, Physical mechanisms and their mathematical descriptions, in: Z.P. Bazant (Ed.), Math. Model. Creep Shrinkage Concr., Wiley, Chichester, 1988: pp. 63–98.
[57] F. Collins, J.. Sanjayan, Effect of pore size distribution on drying shrinking of alkali-activated slag concrete, Cem. Concr. Res. 30 (2000) 1401–1406. doi:10.1016/S0008-8846(00)00327-6.
[58] B.S. Gebregziabiher, R. Thomas, S. Peethamparan, Very early-age reaction kinetics and microstructural development in alkali-activated slag, Cem. Concr. Compos. 55 (2015) 91–102. doi:10.1016/j.cemconcomp.2014.09.001.